

## 3.4

Normalized brain volume  
and white matter  
hyperintensities as  
determinants of cerebral blood  
flow in Alzheimer's disease

Marije R. Benedictus, Maja A.A. Binnewijzend, Joost P.A. Kuijer,  
Martijn D. Steenwijk, Adriaan Versteeg, Hugo Vrenken, Philip Scheltens,  
Frederik Barkhof, Wiesje M. van der Flier, Niels D. Prins

Submitted

## ABSTRACT

**Purpose:** Patients with Alzheimer's disease (AD) have a lower cerebral blood flow (CBF) compared to the general elderly population. It is still not fully understood whether this decreased CBF reflects neurodegeneration, or rather is the consequence of comorbid cerebral small vessel disease (SVD). We aimed to investigate the independent associations of normalized brain volume (NBV) and white matter hyperintensity (WMH) volume with CBF.

**Methods:** We included 129 patients with AD (age  $66 \pm 7$  years, 53%female) and 81 controls (age  $65 \pm 6$  years, 41%female). CBF was measured with pseudo-continuous arterial spin labelling (PCASL) at 3T for whole brain and in partial volume corrected (PVC) cortical and white matter maps. We used linear regression analysis, corrected for age and sex, to investigate independent associations for NBV and WMH volume with CBF.

**Results:** In AD patients, smaller NBV was associated with lower whole brain ( $St\beta:0.28;p<0.01$ ), cortical ( $St\beta:0.27;p<0.01$ ) and white matter CBF ( $St\beta:0.18;p<0.05$ ). In addition, larger WMH volume in AD patients was also associated with lower whole brain ( $St\beta:-0.21;p<0.05$ ) and cortical CBF ( $St\beta:-0.23;p<0.05$ ). In controls, NBV was not associated with CBF, but larger WMH volume tended to be associated with lower whole brain and cortical CBF when NBV and WMH were simultaneously entered in the model (respectively  $St\beta:-0.24$  and  $St\beta:-0.25$ ; both  $p=0.06$ ).

**Conclusion:** Our results indicate that in AD, lower CBF reflects the combined disease burden of both neurodegeneration and SVD. Both processes are assumed to contribute to AD and CBF as measured using PCASL may be a final common pathway.

## INTRODUCTION

Patients with Alzheimer's disease (AD) have a lower cerebral blood flow (CBF) than age-matched controls.<sup>1,2</sup> The decreased CBF is generally considered to be a reflection of the underlying neurodegenerative process that is characterized by amyloid plaques and neurofibrillary tangles and eventually leads to brain atrophy.<sup>3</sup>

Lower CBF in AD patients may not only relate to neurodegeneration however, but may also be associated with underlying cerebrovascular disease. In particular cerebral small vessel disease (SVD) is known to be highly prevalent in patients with AD. White matter hyperintensities (WMH) of presumed vascular origin are an MRI marker reflecting the presence of SVD.<sup>4</sup> WMH are assumed to result from ischemia and they are more prevalent in patients with AD compared to the general elderly population.<sup>5</sup> Previous studies have shown that WMH are associated with lower CBF as well.<sup>6-8</sup>

CBF can be measured by arterial spin labelling (ASL); a functional MRI technique that uses magnetically labelled arterial blood water as an endogenous tracer.<sup>9</sup> The pseudo-continuous variant of ASL (PCASL) uses a multitude of millisecond-long pulses in order to achieve a high labelling efficiency and effective compensation of magnetization transfer effects.<sup>10</sup>

Both neurodegeneration and SVD are common in patients with AD, but to our knowledge, no previous studies investigated how these processes contribute to decreased CBF in AD. Our aim was to explore whether independent relationships exist between NBV (neurodegeneration) or WMH (SVD) on the one hand and CBF on the other hand. We hypothesized that the lower CBF in AD is not only reflective of the neurodegenerative process, but that CBF may be even further decreased when SVD is present. The well-characterized Amsterdam Dementia Cohort with PCASL measurement allowed us to investigate the determinants of CBF in AD patients and controls.

## METHODS

### Subjects

Subjects for this study were drawn from the memory clinic based Amsterdam Dementia Cohort. From October 2010-June 2012 we obtained MRI scans with PCASL in 132 controls and 149 patients with AD. All subjects underwent an extensive dementia screening, including medical history, neurological and physical examination, cognitive assessment and brain MRI. Presence of hypertension, hypercholesterolemia and diabetes mellitus were determined based on self-reported medical history and medication

use. Smoking status was defined as never, former or current. Blood pressures were measured manually using a sphygmomanometer. The diagnosis 'probable AD' was made according to the NINCDS-ADRDA criteria, by consensus of a multidisciplinary team and all patients fulfilled the core clinical criteria of the NIA-AA.<sup>11, 12</sup> The control group consisted of subjects who presented with cognitive complaints, but for whom clinical investigations were normal and criteria for mild cognitive impairment,<sup>13</sup> dementia, or any other neurologic or psychiatric disorder were not met. The ethical review board of the VU University Medical Center approved the study. We obtained informed consent from all patients to use their clinical data for research purposes.

We excluded 4 controls and 4 patients with AD as they had structural brain lesions, such as tumours or trauma. One AD patient was excluded because of hemochromatosis. Pre-processing of PCASL images failed in 2 controls and 7 AD patients. WMH segmentation failed in 5 subjects (3 controls and 1 AD patient) and 8 subjects (1 control and 7 AD patients) were excluded because of movement artefacts. This resulted in a total of 129 patients with AD. In order to have groups with comparable age we excluded 41 younger controls, resulting in a total of 81 age-matched controls.

## MRI protocol

MRI of the brain was acquired on a 3T whole body MR system (Signa, HDxt, General Electric Medical Systems, Milwaukee, WI, USA), using an 8-channel phased-array head coil. The MRI protocol included a sagittal 3D T1-weighted sequence (IR-FSPGR, repetition time [TR]:7.8ms, echo time [TE]:3ms, inversion time [TI]:450ms, flip angle:12°, voxel size:1.0x0.9x0.9mm); a sagittal 3D fluid-attenuated inversion-recovery (FLAIR: TR:8000ms, TE:123.6ms, TI:2350ms, voxel size:1.0x1.0x1.0mm) an axial 2D T2\* gradient-echo with an echo-planar read-out (EPI: TR:5300ms, TE:25ms, voxel size:1.0x0.5x0.5mm); and an axial 2D proton density/T2-weighted fast spin echo (PD-T2: TE:20/112ms, TR:8680ms, voxel size:1.0x0.5x0.5mm). PCASL perfusion images (3D-FSE acquisition with background suppression, post-label delay:2.0s, TR:4.8s, TE:9ms, spiral readout:8 arms x 512 samples; voxel size:1.0x1.7x1.7mm) were calculated using a single compartment model<sup>14</sup> after the subtraction of labelled images from control images. Binnewijzend et al.<sup>2</sup> provides a more detailed description of the ASL sequence.

## PCASL cerebral blood flow measures

After correcting T1-weighted and PCASL images for gradient non-linearities in all three directions, data-analyses were carried out using FSL (version 4.1.9; <http://www.fsl.fmrib.ox.ac.uk/>).

fmrib.ox.ac.uk/fsl). Pre-processing of T1-weighted images consisted of removal of non-brain tissue,<sup>15</sup> linear registration to standard space<sup>16</sup> and tissue segmentation<sup>17</sup> yielding partial volume estimates. PCASL images were linearly registered to the brain-extracted T1-weighted images. Partial volume estimates were transformed to the ASL data space and used in a regression algorithm<sup>18</sup> using a Gaussian kernel of 9.5mm full width at half maximum, to create partial volume corrected (PVC) cortical and white matter CBF maps. Mean whole brain CBF was calculated using the segmented brain mask. Mean cortical and white matter CBF were calculated using the partial volume estimates as a weighting factor. CBF was defined in ml/100g/min.

### Normalized brain volumes

NBV (mL) was estimated with the SIENAX software tool,<sup>15</sup> part of FSL, using optimized brain extraction tool (BET) options as described previously.<sup>19</sup> In order to avoid lesion-associated segmentation biases, prior to segmentation lesions were filled with intensities of the normal appearing white matter using the automated lesion-filling technique LEAP.<sup>20</sup>

### White matter hyperintensities

WMHs were segmented using a locally developed *k* Nearest Neighbour algorithm<sup>21</sup> based on previous work.<sup>22</sup> In short, this algorithm uses FLAIR and T1 tissue intensity, spatial information and tissue priors to compare the brain voxels of a newly presented dataset to a collection of manually labelled examples in a feature space. Based on the most similar examples, the probability of a voxel being a lesion is computed and thresholded to obtain a binary lesion segmentation. Importantly, the training set for automated lesion segmentation was generated on images acquired with the same scanner and pulse sequences as those in the present study. All segmentations were visually inspected, resulting in the exclusion of 7 scans with movement artefacts. WMH volumes (in milliliter, mL) were normalized for head size by multiplying the volumes by a scaling factor, derived from the SIENAX estimation.

### Other MRI measures

Left and right hippocampal volumes (mL) were quantified using FSL FIRST (FMRIBs Integrated registration and segmentation tool).<sup>23</sup> All segmentations were visually inspected. Hippocampal volumes were normalized for head size by multiplying the volumes by the SIENAX derived scaling factor. For analytical purposes, left and right

hippocampal volumes were summed. Cerebral microbleeds were visually assessed and defined as small round foci of hypointense signal, up to 10mm in brain parenchyma on T2\*-weighted images. Microbleed count was dichotomized as present or absent. Lacunes (of presumed vascular origin) were defined as deep lesions (3-15mm), with CSF-like signal on all sequences; they were scored as present or absent.

## Data analysis

Statistical analyses were performed using SPSS (version 20; SPSS, Chicago, Ill., USA ). As WMH volumes were not normally distributed, we used log-transformed values. Differences in baseline characteristics between groups were investigated with student t-test for continuous variables and  $\chi^2$  test for dichotomous variables. Differences in CBF between groups were analysed using one-way ANOVA, corrected for age and sex. Linear regression analysis was carried out to investigate the associations of NBV and WMH (independent) with CBF (dependent). All models were adjusted for age and sex. In model I we investigated the univariate associations of NBV or WMH with CBF. In model II NBV and WMH were simultaneously entered. Model III consisted of model II, with additional adjustment for hippocampal volume, microbleed presence and lacune presence. Linear regression analyses were stratified for diagnosis, to estimate the effects for controls and AD patients separately.

## RESULTS

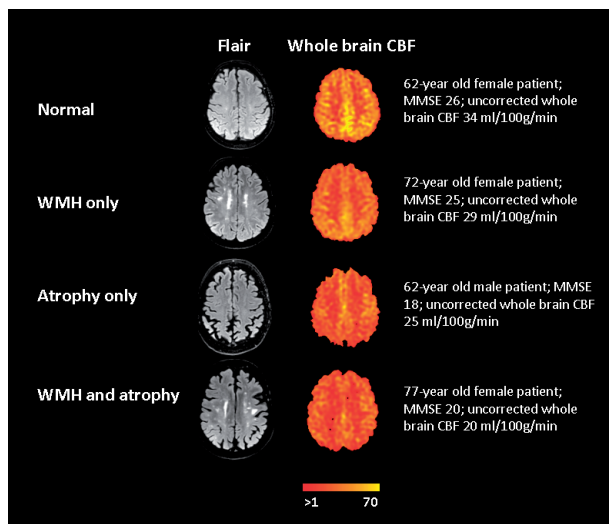


**Figure 1.** Examples of Flair scans and uncorrected whole brain CBF maps of four patients with Alzheimer's disease with different degrees of atrophy and white matter hyperintensities. Abbreviations: CBF:cerebral blood flow; WMH:white matter hyperintensities; MMSE:Mini mental state examination.

**Table 1.** Patient characteristics.

	Controls (n=81)	AD patients (n=129)
<b>Demographics</b>		
Age, yrs	65±6	66±7
Sex (%Female)	33(41%)	69(53%)
MMSE	28±2	21±5 <sup>a</sup>
<b>Vascular risk factors</b>		
Hypertension	16(20%)	32(25%)
Hypercholesterolemie	5(6%)	11(8%)
Diabetes Mellitus	5(6%)	7(5%)
Smoking status		
Never	36(46%)	60(48%)
Former	37(47%)	46(37%)
Current	6(8%)	20(16%)
Systolic BP, mmHg	139±19	144±19 <sup>a</sup>
Diastolic BP, mmHg	85±11	88±11
<b>MRI characteristics</b>		
Normalized brain volume, mL	1430.5±81.7	1368.5±72.3 <sup>a</sup>
Hippocampal volume (left&right), mL	10.0±1.1	8.7±1.2 <sup>a</sup>
WMH volume, (inter-quartile range), mL	median 5.2(3.7; 8.1)	10.9(6.7;19.8) <sup>a</sup>
Microbleed presence	17(21%)	40(31%)
Lacune presence	3(4%)	7(5%)

Data are represented as mean±SD, number of patients with variable present (%), or median (inter-quartile range). Group comparisons used Student t-test for continuous variables and  $\chi^2$ -test for categorical variables. AD: Alzheimer's disease; MMSE: Mini mental state examination; BP: blood pressure; NBV: normalized brain volume, WMH: white matter hyperintensities. Availability for incomplete data in controls: MMSE:79/81, BP:78/81, smoking status:79/81; and in AD patients: BP:125/129, smoking status:126/129, microbleeds:127/129. <sup>a</sup>p<0.01.

Table 1 gives the patient characteristics by group, showing effective matching for age and sex. Systolic blood pressure was higher in AD patients (p<0.01), but all other vascular risk factors were comparable. AD patients had smaller NBVs, smaller hippocampal volumes and larger WMH volumes compared to controls (all p<0.01). There were no differences in the prevalence of microbleeds or lacunes. Compared to controls, AD

patients had a 14% lower CBF in whole brain; a 12% lower PVC cortical CBF and a 13% lower PVC white matter CBF (table 2, all  $p < 0.01$ ).

**Table 2.** Cerebral blood flow for controls and patients with AD.

	Controls	AD patients
Uncorrected whole brain CBF	31.7±5.7	27.3±5.8 <sup>a</sup>
Partial volume corrected cortical CBF	47.3±8.3	41.8±9.2 <sup>a</sup>
Partial volume corrected white matter CBF	25.7±4.9	22.3±4.8 <sup>a</sup>

Data are means±SD in mL/100g/min. Results were adjusted for age and sex. AD: Alzheimer's disease; CBF: cerebral blood flow. <sup>a</sup> $p < 0.01$ .

**Table 3.** Associations of normalized brain volumes and white matter hyperintensities with cerebral blood flow.

	Controls			AD patients		
	CBF (ml/100g/min)			CBF (ml/100g/min)		
	Uncorrected whole brain	PVC cortical	PVC white matter	Uncorrected whole brain	PVC cortical	PVC white matter
Model I						
NBV	0.01	0.00	-0.00	0.28 <sup>a</sup>	0.27 <sup>a</sup>	0.18 <sup>b</sup>
WMH	-0.21	-0.22	-0.11	-0.21 <sup>b</sup>	-0.23 <sup>b</sup>	-0.11
Model II						
NBV	0.06	0.06	0.03	0.29 <sup>a</sup>	0.28 <sup>a</sup>	0.19 <sup>b</sup>
WMH	-0.24 <sup>c</sup>	-0.25 <sup>c</sup>	-0.12	-0.23 <sup>b</sup>	-0.24 <sup>b</sup>	-0.12
Model III						
NBV	0.06	0.05	0.05	0.28 <sup>b</sup>	0.27 <sup>a</sup>	0.20 <sup>b</sup>
WMH	-0.23 <sup>d</sup>	-0.23 <sup>d</sup>	-0.12	-0.24 <sup>b</sup>	-0.25 <sup>a</sup>	-0.12

Standardized regression coefficients are displayed to allow for direct comparison of each variables' contribution. AD: Alzheimer's disease; CBF: cerebral blood flow, PVC: partial volume corrected; NBV: normalized brain volume; WMH: white matter hyperintensities.

Model I: NBV or WMH univariate; adjusted for age and sex. Model II: NBV and WMH simultaneously; adjusted for age and sex. Model III: adjusted for age, sex, hippocampal volume, presence of microbleeds and presence of lacunes.

<sup>a</sup> $p < 0.01$ . <sup>b</sup> $p < 0.05$ . <sup>c</sup> $p = 0.06$ . <sup>d</sup> $p = 0.08$ .

Table 3 gives the associations of NBV and WMH with CBF by group. In AD patients, smaller NBV was associated with lower whole brain CBF, PVC cortical CBF and PVC white matter CBF. In addition, in AD patients, larger WMH volume was associated with lower whole brain CBF and PVC cortical CBF, but not with PVC white matter CBF. When NBV and WMH were simultaneously entered (model II) these results remained essentially unchanged. Additional adjustment for hippocampal volume, presence of microbleeds and presence of lacunes did not change these results (model III). Examples of whole brain CBF maps of four AD patients with different grades of atrophy and WMH are given in figure 1.

In controls, NBV was not associated with CBF. These results remained essentially unchanged when NBV and WMH were simultaneously entered (model II), or after additional adjustment for hippocampal volume, presence of microbleeds and presence of lacunes (model III). WMH volume was not significantly associated with CBF in age and sex adjusted models (model I), but when we simultaneously entered NBV and WMH in the model (model II), larger WMH volume tended to be associated with lower whole brain CBF and PVC cortical CBF (both  $p=0.06$ ). Additional adjustment for hippocampal volume, microbleed and lacune presence (model III) slightly attenuated these tendencies. Figure 2 shows the association of NBV with whole brain CBF and the associations of WMH with whole brain CBF by group.

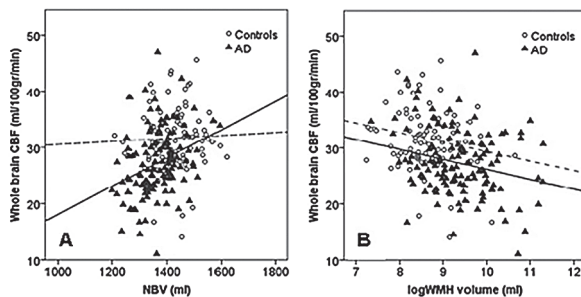


**Figure 2.** A: association of normalized brain volume (NBV) with whole brain cerebral blood flow (CBF) for controls and patients with Alzheimer’s disease (AD). B: association of log-transformed normalized white matter hyperintensity (WMH) volume with whole brain cerebral blood flow (CBF) for controls and patients with AD.

## DISCUSSION

In the present paper we combined quantitative measurement of NBV and WMH volume with quantification of CBF as measured using PCASL. In AD patients, smaller NBVs and larger WMH volumes were both, independently, associated with a lower CBF. In controls, NBV was not associated with CBF, but larger WMH volume tended to be associated

with a lower CBF. The frequently observed decreased CBF in AD patients appears to be determined by both neurodegeneration and SVD. CBF as measured using PCASL may be a final common pathway and as such, reflect total disease burden in patients with AD.

To our knowledge, we are the first to investigate associations of NBV and WMH with CBF as measured using PCASL in a well-characterized set of AD patients and controls. In the present study our control group consisted of subjects who presented with subjective complaints at our memory clinic. This may be considered a limitation, as it has previously been shown that the presence of subjective memory complaints may predict incident AD.<sup>24</sup> However, our measures of interest (NBV, WMH and CBF) all differed between AD patients and controls in expected ways. Furthermore, if anything, we would have underestimated between group differences. Another limitation is that our study had a cross-sectional design. A longitudinal design could give more insight into the still largely unknown order in which neurodegeneration, SVD and decreased CBF occur.

In AD patients, we found that smaller NBVs and larger WMH volumes were both associated with lower CBF. We did not only find an association for NBV with whole brain CBF, but also with PVC cortical CBF, in which errors that have been induced by atrophy have been accounted for.<sup>18</sup> To our knowledge, relatively little research has been performed on the determinants of decreased CBF in AD patients. Previous findings of a dissociation between regional CBF decreases and regional brain volume changes led to the suggestion that in AD patients the underlying mechanisms driving decreased CBF and atrophy may diverge.<sup>25</sup> Although in the present study we did not look at regional changes, one might argue that WMH presence may at least in part account for this dissociation. The independency of the associations that we found indicates that even in the presence of severe neurodegeneration, CBF is even lower when additional SVD is present. As we previously showed that CBF was associated with cognition in AD patients,<sup>2</sup> our findings have clinical relevance and may have several implications. In the first place, this study again underlines the importance of the prevention and treatment of modifiable risk factors for vascular disease in AD patients. In addition, it could be worthwhile to attempt to improve CBF, for instance by means of exercise.<sup>26</sup> Most importantly, however, PCASL may provide a new measure for total disease burden in AD. Accumulating evidence suggests that cerebrovascular pathology interacts with AD pathology, not only affecting the risk of AD,<sup>27</sup> but also its course and cognitive symptoms.<sup>28</sup> However, the exact mechanisms are still not well-understood. CBF measured with PCASL may be a final common pathway that reflects the cumulative burden of neurodegeneration and SVD in patients with AD.

In controls, we found associations of comparable effect size between larger WMH volume and lower CBF as in AD. This is in accordance with several previous findings in a variety of populations,<sup>6-8</sup> although contradictory findings have been reported as well.<sup>29</sup> Contrary to AD patients, we found no association between NBV and CBF in controls. To our knowledge there is no previous literature on the association of brain volume with CBF in healthy elderly. However, in patients suffering from vascular pathology, total brain volume, or brain volume expressed as percentage of total intracranial volume (atrophy), was not found to be associated with whole brain CBF.<sup>30, 31</sup> Our findings suggest that in healthy elderly, variability in CBF is not determined by brain volume and/or minimal cerebral atrophy, but rather reflects the burden of SVD.

Overall our results indicate that independent processes contribute to a decreased CBF. In normal cognition, variability in CBF mainly results from the pathological process of SVD. When the process of neurodegeneration has begun and the stage of clinical dementia has been reached, CBF may decrease further as a reflection of the hypometabolic state associated with the neurodegenerative process.<sup>32</sup> We conclude that CBF as measured using PCASL may provide a bridge between neurodegeneration and small vessel disease and offers opportunities for future research regarding both pathological processes in AD.

## ACKNOWLEDGEMENTS

The authors thank Ajit Shankaranarayanan of GE Healthcare for providing the 3D pseudo-continuous ASL sequence that was used to obtain data for this paper. M.R. Benedictus is supported by Stichting Dioraphte. Research of the VUmc Alzheimer center is part of the neurodegeneration research program of the Neuroscience Campus Amsterdam. The VUmc Alzheimer center is supported by Alzheimer Nederland and Stichting VUmc fonds. The clinical database structure was developed with funding from Stichting Dioraphte.

## REFERENCES

1. Alexopoulos P, Sorg C, Forschler A, et al. Perfusion abnormalities in mild cognitive impairment and mild dementia in Alzheimer's disease measured by pulsed arterial spin labeling MRI. *Eur Arch Psychiatry Clin Neurosci* 2012;262:69-77.
2. Binnewijzend MA, Kuijter JP, Benedictus MR, et al. Cerebral blood flow measured with 3D pseudocontinuous arterial spin-labeling MR imaging in Alzheimer disease and mild cognitive impairment: a marker for disease severity. *Radiology* 2013;267:221-230.

3. Jack CR, Jr, Knopman DS, Jagust WJ, et al. Hypothetical model of dynamic biomarkers of the Alzheimer's pathological cascade. *Lancet Neurol* 2010;9:119-128.
4. Wardlaw JM, Smith EE, Biessels GJ, et al. Neuroimaging standards for research into small vessel disease and its contribution to ageing and neurodegeneration. *Lancet Neurol* 2013;12:822-838.
5. Scheltens P, Barkhof F, Valk J, et al. White matter lesions on magnetic resonance imaging in clinically diagnosed Alzheimer's disease. Evidence for heterogeneity. *Brain* 1992;115 ( Pt 3):735-748.
6. Bastos-Leite AJ, Kuijter JP, Rombouts SA, et al. Cerebral blood flow by using pulsed arterial spin-labeling in elderly subjects with white matter hyperintensities. *AJNR Am J Neuroradiol* 2008;29:1296-1301.
7. Schuff N, Matsumoto S, Kmiecik J, et al. Cerebral blood flow in ischemic vascular dementia and Alzheimer's disease, measured by arterial spin-labeling magnetic resonance imaging. *Alzheimers Dement* 2009;5:454-462.
8. Vernooij MW, van der Lugt A, Ikram MA, et al. Total cerebral blood flow and total brain perfusion in the general population: the Rotterdam Scan Study. *J Cereb Blood Flow Metab* 2008;28:412-419.
9. Petersen ET, Zimine I, Ho YC, Golay X. Non-invasive measurement of perfusion: a critical review of arterial spin labelling techniques. *Br J Radiol* 2006;79:688-701.
10. Dai W, Garcia D, de Bazelaire C, Alsop DC. Continuous flow-driven inversion for arterial spin labeling using pulsed radio frequency and gradient fields. *Magnetic resonance in medicine : official journal of the Society of Magnetic Resonance in Medicine / Society of Magnetic Resonance in Medicine* 2008;60:1488-1497.
11. McKhann G, Drachman D, Folstein M, Katzman R, Price D, Stadlan EM. Clinical diagnosis of Alzheimer's disease: report of the NINCDS-ADRDA Work Group under the auspices of Department of Health and Human Services Task Force on Alzheimer's Disease. *Neurology* 1984;34:939-944.
12. McKhann GM, Knopman DS, Chertkow H, et al. The diagnosis of dementia due to Alzheimer's disease: recommendations from the National Institute on Aging-Alzheimer's Association workgroups on diagnostic guidelines for Alzheimer's disease. *Alzheimers Dement* 2011;7:263-269.
13. Petersen RC, Stevens JC, Ganguli M, Tangalos EG, Cummings JL, DeKosky ST. Practice parameter: early detection of dementia: mild cognitive impairment (an evidence-based review). Report of the Quality Standards Subcommittee of the American Academy of Neurology. *Neurology* 2001;56:1133-1142.
14. Buxton RB, Frank LR, Wong EC, Siewert B, Warach S, Edelman RR. A general kinetic model for quantitative perfusion imaging with arterial spin labeling. *Magnetic Resonance in Medicine* 1998;40:383-396.
15. Smith SM. Fast robust automated brain extraction. *HumBrain Mapp* 2002;17:143-155.
16. Jenkinson M, Smith S. A global optimisation method for robust affine registration of brain images. *MedImage Anal* 2001;5:143-156.
17. Zhang Y, Brady M, Smith S. Segmentation of brain MR images through a hidden Markov random field model and the expectation-maximization algorithm. *IEEE TransMedImaging* 2001;20:45-57.

18. Asllani I, Borogovac A, Brown TR. Regression Algorithm Correcting for Partial Volume Effects in Arterial Spin Labeling MRI. *Magnetic Resonance in Medicine* 2008;60:1362-1371.
19. Popescu V, Battaglini M, Hoogstrate WS, et al. Optimizing parameter choice for FSL-Brain Extraction Tool (BET) on 3D T1 images in multiple sclerosis. *Neuroimage* 2012;61:1484-1494.
20. Chard DT, Jackson JS, Miller DH, Wheeler-Kingshott CA. Reducing the impact of white matter lesions on automated measures of brain gray and white matter volumes. *J Magn Reson Imaging* 2010;32:223-228.
21. Steenwijk MD, Pouwels PJ, Daams M, Barkhof F, Vrenken H. Accurate white matter lesion segmentation by k nearest neighbor classification with tissue type priors. *Neuroimage Clinical* 2013;under revision.
22. Anbeek P, Vincken KL, Viergever MA. Automated MS-lesion segmentation by K-nearest neighbor classification. *MIDAS Journal* 2008:1-8.
23. Patenaude B, Smith SM, Kennedy DN, Jenkinson M. A Bayesian model of shape and appearance for subcortical brain segmentation. *Neuroimage* 2011;56:907-922.
24. Geerlings MI, Jonker C, Bouter LM, Ader HJ, Schmand B. Association between memory complaints and incident Alzheimer's disease in elderly people with normal baseline cognition. *Am J Psychiatry* 1999;156:531-537.
25. Luckhaus C, Cohnen M, Fluss MO, et al. The relation of regional cerebral perfusion and atrophy in mild cognitive impairment (MCI) and early Alzheimer's dementia. *Psychiatry Res* 2010;183:44-51.
26. Barnes JN, Taylor JL, Kluck BN, Johnson CP, Joyner MJ. Cerebrovascular reactivity is associated with maximal aerobic capacity in healthy older adults. *J Appl Physiol* 2013;114:1383-1387.
27. van der Flier WM, Middelkoop HA, Weverling-Rijnsburger AW, et al. Interaction of medial temporal lobe atrophy and white matter hyperintensities in AD. *Neurology* 2004;62:1862-1864.
28. Brickman AM, Honig LS, Scarmeas N, et al. Measuring cerebral atrophy and white matter hyperintensity burden to predict the rate of cognitive decline in Alzheimer disease. *Arch Neurol* 2008;65:1202-1208.
29. Zhang Q, Stafford RB, Wang Z, Arnold SE, Wolk DA, Detre JA. Microvascular perfusion based on arterial spin labeled perfusion MRI as a measure of vascular risk in Alzheimer's disease. *J Alzheimers Dis* 2012;32:677-687.
30. Appelman AP, van der Graaf Y, Vincken KL, et al. Total cerebral blood flow, white matter lesions and brain atrophy: the SMART-MR study. *J Cereb Blood Flow Metab* 2008;28:633-639.
31. van Es AC, van der Grond J, ten Dam VH, et al. Associations between total cerebral blood flow and age related changes of the brain. *PLoS One* 2010;5:e9825.
32. Jueptner M, Weiller C. Review: does measurement of regional cerebral blood flow reflect synaptic activity? Implications for PET and fMRI. *Neuroimage* 1995;2:148-156.